PROCEEDINGS OF SCIENCE

Ultra-Peripheral J/ψ Production at Forward Rapidities in Pb-Pb Interactions

K. L. Graham for the ALICE Collaboration*
School of Physics and Astronomy, The University of Birmingham, Birmingham, UK, B15 2TT
E-mail: katie.leanne.graham@cern.ch

Ultra-peripheral Pb-Pb collisions, in which the two nuclei pass close to each other at an impact parameter greater than the sum of their radii, provide information about the initial state of nuclei. In particular, J/ψ production in such collisions proceeds by photon-gluon interactions, and gives access to nuclear parton density functions. The ALICE collaboration has published measurements of ultra-peripheral J/ψ production in Run 1 of the Large Hadron Collider (LHC) in the rapidity range -3.6 < y < -2.6, and has obtained a substantially larger data set in 2015 from LHC Run 2. In this proceedings, the ALICE results on this topic, including the status of the current analysis, will be reported.

XXIV International Workshop on Deep-Inelastic Scattering and Related Subjects
11-15 April, 2016
DESY Hamburg, Germany

*Speaker.

PoS(DIS2016)191

1. Introduction to ultra-peripheral collisions

In Ultra-Peripheral Collisions (UPC), the projectiles (at the LHC either p or Pb) have an impact parameter greater than the sum of their radii, $b > R_1 + R_2$, as shown in Figure 1. This large separation means that hadronic processes are greatly suppressed, and electromagnetic interactions dominate. Since the photon flux is proportional to the square of the projectile charge, heavy ions in particular act as an abundant source of photons with which to probe the structure of the other projectile. Photons produced from lead nuclei, which have radii of ~ 7 fm, have very low virtualities of ~ 30 MeV, and can be considered quasi-real.

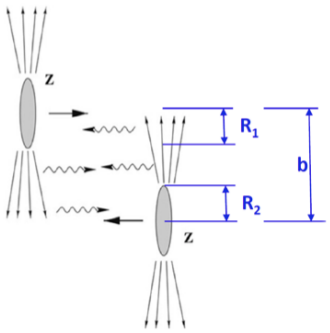

Figure 1: Projectiles of radii R passing at an impact parameter b.

In the photoproduction reaction, the photon emitted by one projectile couples to a vector meson such as the J/ψ, as shown in Figure 2. At leading order, the cross section for this process at forward rapidity is proportional to the square of the gluon parton density function,

$$\frac{\mathrm{d}\sigma_{\gamma^* Pb}(t=0)}{\mathrm{d}t} = \frac{16\Gamma_{ee}\pi^3}{3\alpha_{em}M_{J/\psi}^5}\{\alpha_s(Q^2)xG_{Pb}(x,Q^2)\}^2, \tag{1.1}$$

where t is the four-momentum squared transferred to the nucleus, Γ_{ee} is the decay width to electrons, α_{em} and α_s are the electromagnetic and strong couplings respectively, $x = M_{J/\psi}^2/W_{\gamma p}$ is the fraction of the nucleon momentum carried by the gluons, $M_{J/\psi}$ is the mass of the J/ψ, $W_{\gamma p}$ is the photon-proton centre-of-mass energy, and the nuclear gluon distribution $G_{Pb}(x,Q^2) = g_p(x,Q^2) \times R_g^{Pb}(x,Q^2)$ is the product of the free gluon parton density function g_p and the gluon modification R_g^{Pb} [1]. The J/ψ provides a hard scale $Q^2 \sim M_{J/\psi}^2/4 \sim 2.5$ GeV^2.

The values of Bjorken-x probed in Pb-Pb collisions are given by

$$x = \frac{M_{J/\psi}}{\sqrt{s_{NN}}}\exp(\pm y), \tag{1.2}$$

and the energy of the photon by

$$\omega = \frac{M_{J/\psi}}{2}\exp(\mp y), \tag{1.3}$$

where $\sqrt{s_{NN}}$ is the nucleon-nucleon centre-of-mass energy and y is the rapidity.

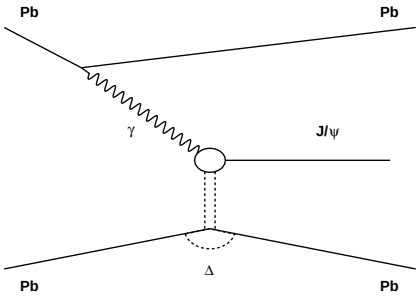

Figure 2: The leading order Feynman diagram for photoproduction of a J/ψ meson in a UPC Pb-Pb interaction.

The decay products of the J/ψ, in this case a $\mu^+\mu^-$ pair, are measured in the ALICE muon arm, which is located at forward rapidity ($-4.0 < y < -2.5$). There are two possible x values for each energy since in Pb-Pb there is an ambiguity as to which nucleus was the photon source. If the photon was emitted by the ion travelling towards the muon arm then it will have a higher energy and access gluons with a lower Bjorken-x. This leads to two components for the cross section for this process,

$$\frac{\mathrm{d}\sigma_{UPC}}{\mathrm{d}y} = n(\omega_1)\sigma_{\gamma T}(\omega_1) + n(\omega_2)\sigma_{\gamma T}(\omega_2), \tag{1.4}$$

where $n(\omega)$ is the flux, from a lead ion, of photons with energy ω, and $\sigma_{\gamma T}(\omega)$ is the cross section for the photoproduction of J/ψ off the target lead ion.

2. The ALICE detector

ALICE is an experiment at the LHC that is optimised for collisions of lead ions, and consists of various sub-detectors, shown in Figures 3 and 4. The detector is described in [2], and its performance in [3]. Since this analysis focuses on exclusive production of J/ψ decaying into muons in the forward direction, little of the central barrel is used, except to veto activity in this region ($|\eta| < 0.9$), which is not expected alongside forward muons in exclusive production. Pseudorapidity is defined as $\eta = -\frac{1}{2}\ln(\tan(\frac{\theta}{2}))$, where θ is the angle from the interaction point relative the beam axis. The VZERO counters, which are two pairs of scintillator arrays placed on either side of the interaction point, at $2.8 < \eta < 5.1$ (V0A) and $-3.7 < \eta < -1.7$ (V0C), are used to require that there are no more than two hits in the direction of the muon spectrometer (V0C) and that there are no hits in the opposite direction (V0A). Beyond the V0C there is a $10\lambda_I$ thick absorber to filter out particles other than muons, and then a muon spectrometer consisting of 10 planar cathode-pad multi-wire-proportional-chamber trackers, two of which are contained within a 0.67 T dipole magnet to enable momentum measurement, in the pseudorapidity range $-4.0 < \eta < -2.5$. Following this is an iron wall and then a muon triggering system. There are also two Zero-Degree Calorimeters (ZDCs) at about 110 m either side of the interaction point, which detect very forward neutrons. The ALICE Diffractive (AD) detectors were added between LHC Runs 1 and 2, and are double layer scintillation counters around the beamline 16 m or 19 m from the interaction point.

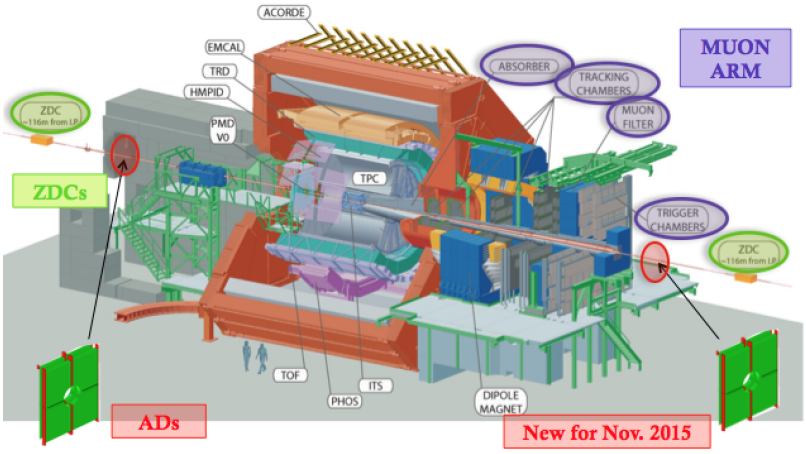

Figure 3: The ALICE detector.

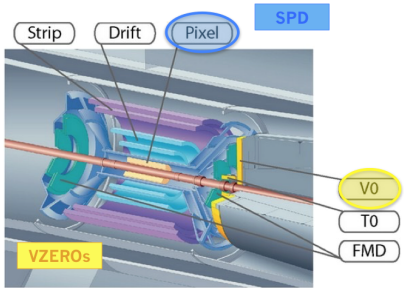

Figure 4: A close-up view of the ALICE inner detectors.

3. Run 1 results

During LHC Run 1, in UPC Pb-Pb collisions at $\sqrt{s_{NN}} = 2.76$ TeV, coherent J/ψ photoproduction was measured in two rapidity regions, as shown in Figure 5. At mid-rapidity ($|y| < 0.9$, which corresponds to $x \sim 10^{-3}$) the cross section was measured to be $\mathrm{d}\sigma^{coh}_{J/\psi}/\mathrm{d}y = 2.38^{+0.34}_{-0.24}$ (stat.+syst.) mb [4]. At forward rapidity the cross section was $\mathrm{d}\sigma^{coh}_{J/\psi}/\mathrm{d}y = 1.00 \pm 0.18$ (stat.) $^{+0.24}_{-0.26}$ (syst.) mb [5] ($-3.6 < y < -2.6$, with $\sim 90\%$ of this sample having Bjorken-$x \sim 10^{-2}$ and the rest having $x \sim 10^{-5}$). These measurements can be compared with various models which treat the photonuclear interaction in different ways. For mid-rapidity, where there was better discrimination between predictions. The result suggested that partonic models including moderate nuclear gluon shadowing, such as AB-EPS09 [6], are preferred.

4. J/ψ signal extraction in Run 2

In 2015, three weeks of Pb-Pb data were taken at an energy of $\sqrt{s_{NN}} = 5.02$ TeV. This higher $\sqrt{s_{NN}}$ allows access to higher $W_{\gamma p}$ values, measured in the same rapidity interval, than in Run 1, as can be seen from the equations in Section 1. Using triggers specifically designed for UPC, events

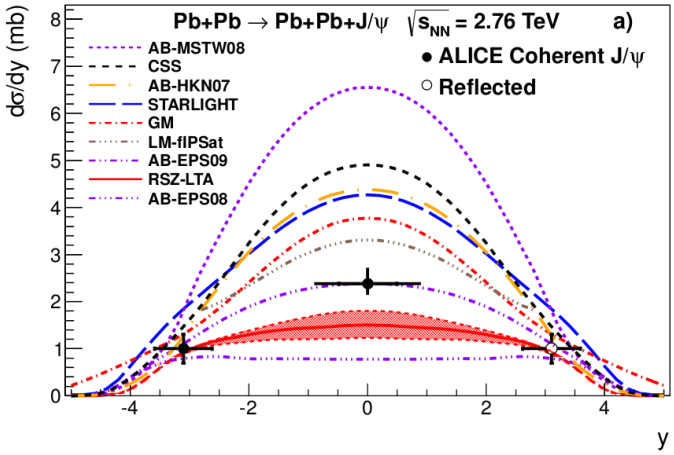

Figure 5: Cross sections for coherent J/ψ measured by ALICE in UPC, shown with various theoretical predictions.

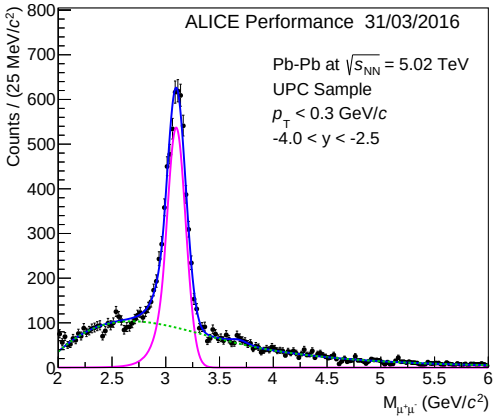

Figure 6: Dimuon invariant mass with a fit to the J/ψ peak.

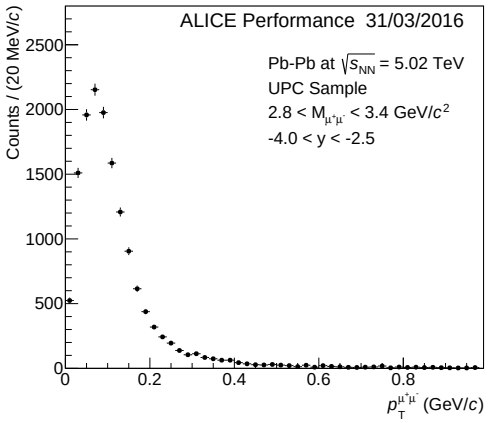

Figure 7: Dimuon transverse momentum spectrum.

were selected to be exclusive (*i.e.* only two muons were detected), with no nuclear breakup and a transverse momentum cut of $p_T^{\mu^+\mu^-} < 0.3$ GeV/c in order to select an enriched sample of coherently produced J/ψ. The invariant mass spectrum is shown in Figure 6, and the p_T spectrum in the J/ψ mass range is shown in Figure 7. After some track quality selections, there were around 50 times as many J/ψ candidates as in the Run 1 analysis.

This increase in statistics allows cross sections to be measured in 3 bins of forward rapidity, potentially giving better discrimination between theoretical models than was possible in Run 1. So far, cross section predictions have been made by Guzey *et al.* [7], Thomas *et al.* [8], and STARLIGHT [9].

5. Forward neutron production

The low- and high-energy contributions to the cross section, shown in Equation 1.4, are dif-

ficult to disentangle. Since the low-x (high photon energy) contribution is the most interesting, a method was devised to achieve separation using forward neutron emission, which can be measured using the ZDC detectors. The idea behind this is that, separately from the coherent J/ψ production we are interested in, the nuclei can photodissociate, resulting in emission of neutrons. Using the ZDCs, events can be categorised into 0n0n (*i.e.* no neutrons in the A-side ZDC, and no neutrons in the C-side ZDC), 0nXn, Xn0n, and XnXn (where X $>$ 0), which each have different proportions on low-x and high-x J/ψ photoproduction. This is because the flux of high-energy photons decreases faster with the impact parameter b than the flux of low-energy photons, and the probability of photodissociation also decreases with b. Selecting events with neutrons in the ZDC (*i.e.* events in which photodissociation has taken place) thus gives a sample with lower b and so a larger ratio of low-x to high-x events than the sample with no neutrons. See [10] and [7] for a more detailed explanation.

6. Summary

Vector meson photoproduction in ultra-peripheral heavy ion collisions is sensitive to gluon distribution functions. ALICE has previously published results on this topic from LHC Run 1, but there has been a large increase in statistics from Run 2, particularly for the J/ψ at forward rapidity. This allows much more detailed analyses to be carried out, including separation of the cross section into low- and high-x contributions. This analysis is well underway, with results expected soon.

References

[1] A. Adeluyi and C. A. Bertulani, *Gluon distributions in nuclei probed at energies available at the CERN Large Hadron Collider*, *Phys. Rev. C* **84** (2011) 024916.

[2] K. Aamodt *et al*, *The ALICE experiment at the CERN LHC*, *JINST3* (2008) S08002.

[3] B. B. Abelev *et al*, *Performance of the ALICE Experiment at the CERN LHC*, *Int. J. Mod. Phys. A***29** (2014) 1430044.

[4] E. Abbas *et al*, *Charmonium and e^+e^- pair photoproduction at mid-rapidity in ultra-peripheral Pb-Pb collisions at $\sqrt{s_{NN}} = 2.76$ TeV*, *Eur. Phys. J. C* **73** (2013) 2617.

[5] B. Abalev *et al*, *Coherent J/ψ photoproduction in ultra-peripheral Pb-Pb collisions at $\sqrt{s_{NN}} = 2.76$ TeV*, *Phys. Lett. B* **718** (2013) 1273.

[6] A. Adeluyi and C. A. Bertulani, *Constraining gluon shadowing using photoproduction in ultraperipheral pA and AA collisions*, *Phys. Rev. C* **85** (2012) 044904.

[7] V. Guzey, E. Kryshen and M. Zhalov, *Coherent photoproduction of vector mesons in heavy ion ultraperipheral collisions: update for Run 2 at the LHC*, (2016) arXiv:1602.01456.

[8] J. Thomas *et al*, *Parton distribution functions probed in ultraperipheral collisions at the CERN Large Hadron Collider*, (2016) arXiv:1603.01919.

[9] http://starlight.hepforge.org

[10] A. J. Baltz, S. R. Klein and J. Nystrand, *Coherent Vector-Meson Photoproduction with Nuclear Breakup in Relativistic Heavy-Ion Collisions*, *Phys. Rev. Lett.* **89** (2002) 012301.